Engineering and Technology Journal
Journal homepage: https://etj.uotechnology.edu.iq

Synthesized of gallium Nitride/PSi nano thin films using 532 nm wavelength by pulsed laser deposition technique

Abeer R. Abbas[a], Ali A. Alwahib[a], Makram A. Fakhri[a*], Subash C. B. Gopinath[b, c, d], U. Hashim[e]

[a] Laser and Optoelectronics Engineering Dept., University of Technology-Iraq, Alsina'a street, 10066 Baghdad, Iraq.
[b] Center for Global Health Research, Saveetha Medical College & Hospital, Saveetha Institute of Medical and Technical Sciences (SIMATS), Thandalam, Chennai – 602 105, Tamil Nadu, India.
[c] Faculty of Chemical Engineering & Technology & Institute of Nano Electronic Engineering, Universiti Malaysia Perlis (UniMAP), 02600 Arau, Perlis Malaysia.
[d] Department of Technical Sciences, Western Caspian University, Baku AZ 1075, Azerbaijan.
[e] Institute of Nano Electronic Engineering, Universiti Malaysia Perlis, 01000 Kangar, Perlis, Malaysia
*Corresponding author Email: makram.a.fakhri@uotechnology.edu.iq

HIGHLIGHTS

- Grown GAN nanofilm had a hexagonal crystalline structure and high-intensity peak at (002) plane.
- The absorption spectrum of grown GaN film showed a high absorbance at a UV spectrum of 302.88, 435.26 nm
- High-distributed GaN nanostructure was deposited.

ARTICLE INFO

Handling editor: Abdullah k. Abass

Keywords:
Pulsed laser deposition
GaN
Psi
Nanostructure
Thin films

ABSTRACT

The porous silicon (PSi) substrate was accurately synthesized using photoelectrochemical etching. A Nanofilm gallium nitride (GaN) was then precisely deposited on this PSi substrate using pulsed laser deposition (PLD). The x-ray diffraction (XRD) investigation revealed the GaN layer's distinct crystalline structure along the (002) plane, with a precise crystallite size of 21.57 nm. This precision in the deposition process enhanced both the surface morphology and film quality. In the atomic force microscope (AFM), oval particles were evenly distributed across the entire surface, and the RMS of the surface was 27 nm with a 20.63 nm surface roughness. A field emission scanning microscope (FESEM) image of the gallium nitride (GaN) films deposited at a wavelength of 532 nm showed that the GaN material had an evenly covered Psi surface. This reflected the presence of a smooth and even spread of round particles. The cross-sectional area of the GaN sheet had a thickness of 2.92 µm, demonstrating the precision of the deposition technique. The resulting GaN nanofilms demonstrate UV photoluminescence (P.L.), characterized by a wavelength peak of 363.7 nanometers, indicative of the GaN material. In addition, they display a red photoluminescence peak at 723 nanometers, corresponding to the PSi substrate. Under UV-visible light and photoluminescence (P.L.), the optical energy gaps of the GaN nanofilm and the PSi substrate were determined. The PSi substrate exhibited an optical energy gap of 2.1 electron volts, whereas the resulting gallium nitride nanofilms displayed multiple energy band gaps of 3.4 electron volts and 1.7 electron volts.

1. Introduction

In nanotechnology, manufacturing materials with nanostructured compositions has become a focal point in the material science community. Such materials possess at least one dimension at a nanoscale level. Their nanostructures show unique physical and chemical properties compared to bulky materials [1]. Materials give high potential energy, variable band gaps (in the case of metal oxides), strong conductivity, and more as the nanoscale gets closer to the atomic level. On the other hand, nanomaterials are tiny in size and have a large surface area for their bulk [2]. Nanomaterials scientists have devoted a decent effort to examine aspects of manufacturing, material behaviors, and applications. Nanomaterials can be nanoparticles, nanorods, nanosheets, and even monolayers. The business of thin films is crucial in high-tech sectors because they show different performances and modify the surface's nature. For instance, nanocoating can change the surface from hydrophobic to hydrophilic. The characteristics of these

http://doi.org/10.30684/etj.2024.145816.1667
Received 25 March 2024; Received in revised form 29 April 2024; Accepted 14 May 2024; Available online 24 July 2024
2412-0758/University of Technology-Iraq, Baghdad, Iraq

nanomaterials are directly affected by many factors, such as the production process, phase (whether amorphous or crystalline), surface nature (hydrophilic or hydrophobic), and geometrical shape [3].

Nanomaterials are used in various applications, such as catalysis, gas sensors, environmental adsorbents, batteries, and beyond. Some metal oxides in film form have been employed as sensing layers to offer sufficient surface-to-volume ratios for efficient gas-molecule interaction. Unlike nanofilms as sensors, nanostructures can improve the sensors' sensitivity and reaction time or vice versa. The characteristics of these nanomaterials are directly affected by many factors, such as the production process, phase (whether amorphous or crystalline), surface nature (hydrophilic or hydrophobic), and geometrical shape [3]. Nanomaterials can also be used in various applications, such as catalysis, gas sensors, environmental adsorbents, batteries, and beyond. Some metal oxides in film form have been employed as sensing layers to offer sufficient surface-to-volume ratios for efficient gas-molecule interaction. Unlike nanofilms used as sensors, nanostructures can enhance the sensors' sensitivity and reaction time. The atomic structure of the nanomaterials dictates the sensor's performance. Additionally, the size of the sensors allows for adjustments to their selectivity and increases their sensitivity [4].

As sensing devices, nanomaterials have become a significant area of research for improving gas monitoring and management for safety and environmental considerations. Moreover, these sensors are needed to enhance combustion processes in the expanding transportation domain and residential and commercial environments [5].

GaN films have potential applications in optoelectronic devices, leading to numerous studies on their development and properties. Furthermore, GaN films are utilized in high-power and high-temperature electronic equipment [6]. Gallium nitride (GaN) is used in many devices, including but not limited to lasers, visible and ultraviolet (UV) light-emitting diodes (LEDs), solar cells, and sensor materials [7]. Many researchers have studied other substrate types, such as GaAs, Si, and SiC, for the culture of InN, GaN, and AlN and their related complexes. The advantages of GaN growth on silicon substrates—such as affordability, large surface area, and high thermal and electrical conductivity—make it highly attractive. However, producing high-quality epitaxial GaN on silicon substrates faces challenges due to significant differences in lattice structure and thermal expansion coefficients between silicon and GaN [8]. Porous silicon (PSi) consists of tiny filaments and voids. It is made by electro-etching a hydrofluoric acid (H.F.) solution. Its capability to emit visible light in response to photons makes it beneficial in optoelectronics and biology fields [9]. Due to their variable refractive index, high surface-to-volume ratio, and biocompatibility, porous silicon substrates are advantageous for solar cells [10,11]. Layers of PSi are suitable for sensing due to their sponge-like nature and large internal surface area. This material stands out for its affordability, ease of production, and effectiveness in analyzing substances within the pores [12]. As a result, it has demonstrated good performance as a high-absorption coefficient sensor. The porosity, size, and pore structure of porous silicon are defined by the pores, which can be modified by altering the etching parameters [13]. The pulsed laser deposition (PLD) method offers some advantages such as flexibility, ease of operation, and the production of high-quality film structures [14].

In this study, pulsed laser deposition (PLD) was employed using an Nd solid-state laser operating at 532 nm wavelength, with 900 mJ laser energy, under a vacuum pressure of 10−2 Torr. GaN nanomaterials were deposited onto a porous silicon substrate to form a thin film intended for gas sensor applications. The structural, optical, and spectroscopic characteristics of the GaN thin film were investigated for its suitability in gas sensing applications.

2. Theoretical part

2.1 Gallium nitride properties

Gallium nitride (GaN) thin films have recently garnered considerable scientific and industrial interest [15]. Furthermore, nitride-based semiconductors possess a significant direct bandgap. InN, GaN, and AlN have bandgap values of 0.7 to 1.9 eV, 3.4 eV, and 6.1 eV, respectively [16]. The wide range of direct-range gaps associated with blue and UV outputs makes them ideal to be used as optoelectronic devices [17], such as optical detectors, laser diodes, and light-emitting diodes (LEDs) [18]. Moreover, it works with powerful electrical equipment [18]. Multiple types of III-nitride semiconductors can crystallize the mixture of zinc and wurtzite. However, due to its high thermodynamic stability, the former is subject to much investigation. High-temperature and high-frequency applications were implemented with semiconductor III-nitride. For example, at much higher temperatures, the material becomes intrinsic due to the enormous bandgap property of GaN. Nitride III has many desirable qualities, including excellent electron transfer capabilities and high saturation drift velocity [19], atomic solid bonding [14], high collapse fields [19], thermal stability [20], chemical stability [21], and excellent mechanical stability. These characteristics are essential for high-power devices to operate [16]. Due to its mechanical and electrical properties, gallium nitride is a good choice for sensor applications. GaN (gallium nitride) sensors can operate at high temperatures, owing to the material's high melting point. Additionally, GaN exhibits a wide bandgap. The use of inexpensive materials makes GaN impedance sensors cost-effective [22].

2.2 Pulsed laser deposition (PLD) technique

Pulsed laser deposition (PLD) is a technique within physical vapor deposition [23], used to create thin films through several steps: interaction of laser energy with the target material, dynamics of the material plume, deposition of ablated materials onto the substrate, and growth of a thin film on the substrate’s surface. The PLD process is a unique instrument for producing superior films of intricate chemical combinations. More than 200 distinct materials can be deposited using it. Scientists have mainly used this approach as a lab tool to create films of various substances that are often difficult to produce using other techniques [24,25]. The high kinetic energy of the deposited species is another characteristic of PLD, a physical deposition process. Depending on their structure and composition, the target materials experience evaporation, often called ablation, if the laser delivers sufficient energy [26].

3. Experimental work

3.1 Preparation of a porous silicon (PSi) substrate

In this study, the photoelectrochemical etching method was used to create porous silicon. First, the N-type Si wafer (100) was cleaned in the first step using alcohol to remove any contaminants. Then, a silicon wafer was securely placed into the Teflon container, and a 20-ml hydrofluoric acid (40%) was used. Afterward, the experiment utilized a 100 mW laser diode and platinum, operating at a pulsed laser wavelength of 660 nm. After that, the platinum rod was linked to the cathode of a direct-current power source, while the anode was connected to the container of the Teflon base via the metallic side. Finally, a platinum rod was submerged in the solution of H.F., resulting in an applied current of 20 mA. The brief ten-minute duration of laser irradiation proved sufficient for the flawless formation of PSi. Figure 1 illustrates the electrochemical etching induced by the light method. Figure 1a shows a diagram of a photoelectrochemical etching induced by laser system with explanatory marks for each of its parts, and Figure 1b shows a realistic image of porous silicon in gray areas without irradiation with ultraviolet light and pink when irradiated with ultraviolet light.

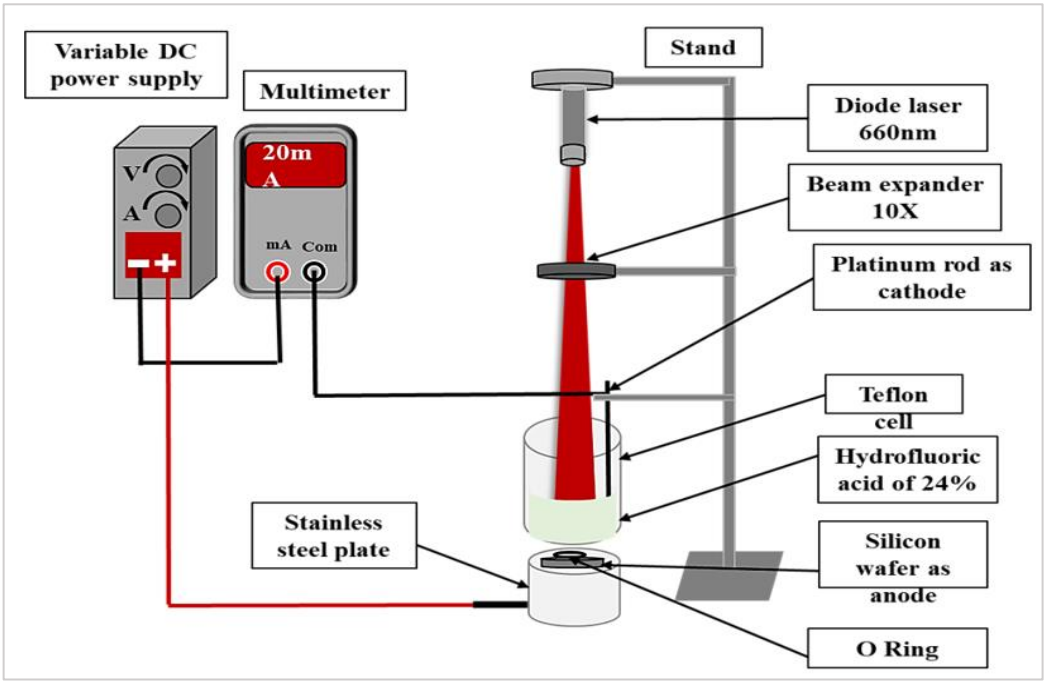

(a)

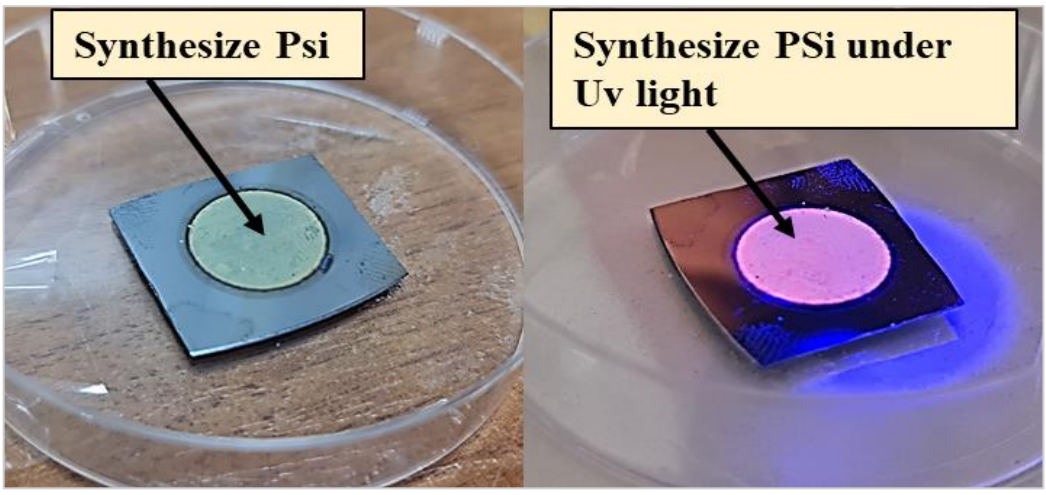

(b)

Figure 1: (a) Photoelectrochemical etching technique to fabricate porous silicon (b) shows a realistic image of porous without and with irradiated by the ultraviolet light

3.2 Preparation of a gallium nitride target

GaN powder was ground using a hydraulic press at a 15 kg/cm^2 pressure to create the GaN pellet. Figure 2 displays a GaN sample weighing 3 grams with a diameter of 2 cm and a thickness of 0.5 cm.

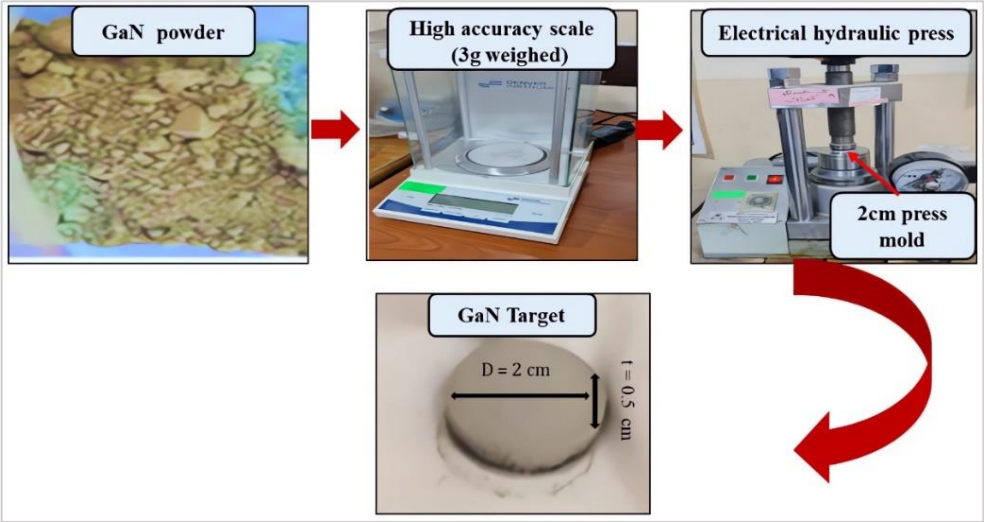

Figure 2: The procedure for producing the GaN pellet

3.3 Fabrication of GaN/Psi by pulsed laser deposition method

Pulsed laser deposition (PLD) made GaN thin films on porous silicon substrates when the vacuum pressure was 10–2 mbar. The Q-switched Nd: YAG pulsed laser was adjusted to emit light at a wavelength of 532 nm, as shown in Figure 3. The duration of each pulse was seven nanoseconds, and the rate at which the pulses were repeated was 3 hertz. The Nd: YAG laser beam was concentrated on a GaN particle of 99.999% purity using 250 pulses. Table 1 displays the parameters utilized in PLD. The following section employed X-ray diffraction (XRD), atomic force microscopy (AFM), and field emission scanning electron microscopy (FESEM) to evaluate GaN/Porous Silicon (100) samples.

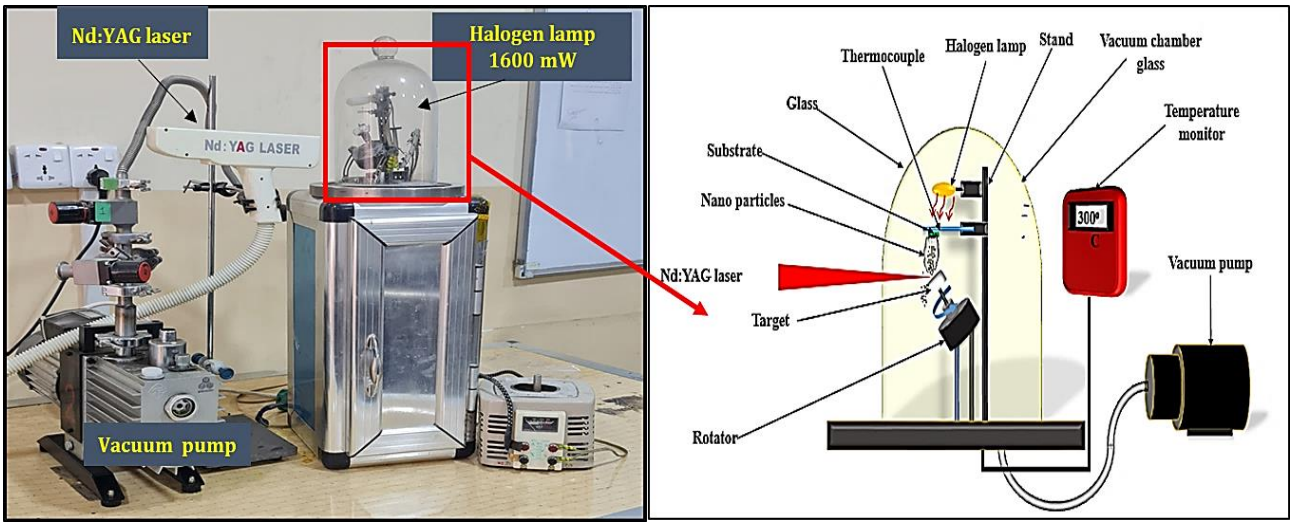

Figure 3: An experimental setup of pulsed laser deposition system to prepare GaN/Psi thin film at 532 nm wavelenght

Table 1: The practical parameters of the PLD method

Laser parameter	The values
Laser wavelength	532 nm
Pulse energy	900 mJ
Pulse duration	Seven ns
Frequency	3 Hz
Power supply	900 v
Substrate temperature	300 ℃

4. Results and discussion

4.1 Structural features

The X-ray results of PSi and gallium nitride nanostructures are shown in Figure 4a,b. The gallium nitride nanostructures were deposited onto the porous silicon substrate using a 532 nm laser. The X-ray diffraction (XRD) patterns of the silicon substrate in Figure 4a exhibit a cut-off at 2θ = 69.62°, which is high and makes it difficult to distinguish other planes. In contrast, the XRD patterns of porous silicon at 2θ = 69.82° display a distinct and intense peak attributed to the (400) plane.

This corresponds to JCPDS (cards NO. 27–1402) and coordinates as described by Sampath [27,28]. Figure 4b displays the GaN nanostructure generated using 900 mJ laser energy at a wavelength of 532 nm. The nanostructure has a hexagonal GaN rise at 2θ = 33.45, 2θ = 33.54, and 2θ = 62.13. These points correspond to reflections from the (002), (002), and (103) planes, respectively, corresponding to JCPDS (cards NO 01-074-0243), according to Kang et al. [29], with an average crystallite size of 21.75 nm, as shown in Table 2. The X-ray diffraction analysis showed that GaN did grow successfully on the used substrates, showing that the method was very effective and pure. The peaks observed in the X-ray diffraction patterns correspond to the characteristic hexagonal structure of GaN [30]. We used the Scherer Equation 1 to determine the size of the crystallites on the Psi substrate and the grown GaN thin film [31].

$$D = 0.94\lambda/\beta \cos\theta \quad (1)$$

where θ is the diffraction angle, β is the full width at half maximum, and λ is the incoming X-ray wavelength (λ = 1.5406 Å). Additionally, the interplanar distance d was calculated using the Equation 2 [32] to provide the results displayed in Table 2:

$$d = n\,\lambda/2\sin\theta \quad (2)$$

where n is the diffraction order, λ is the wavelength of the X-ray (Cu$K\propto$ = 1.54060 A^°), β is the (FWHM)full-width half maximum of the pattern of the X-ray diffraction, θ is the angle of Bragg's in degree, and d is the spacing of the interplanar in A^°, K is a constant, which is assumed to be 0.9.

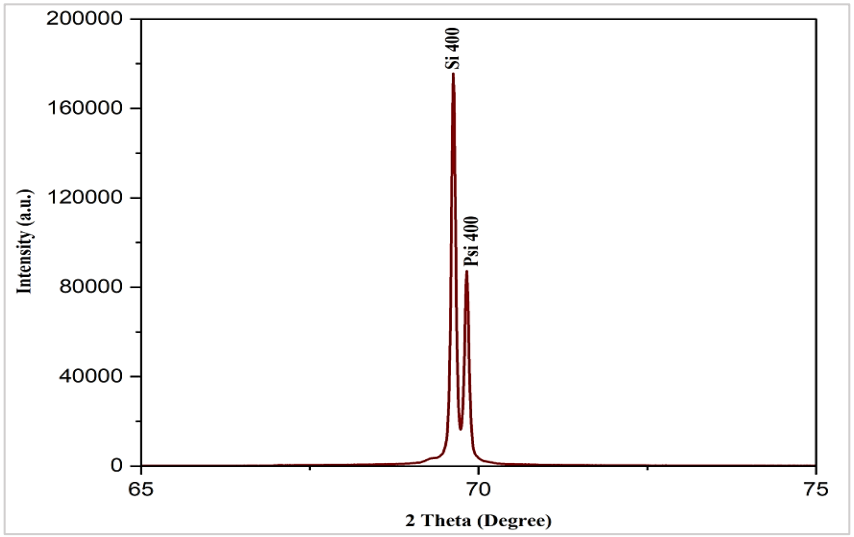

(a)

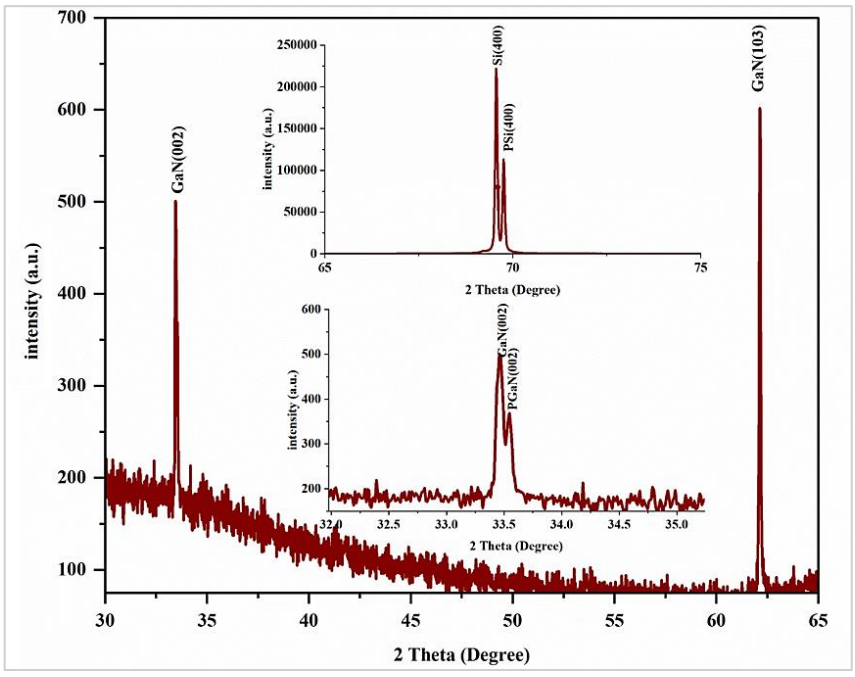

(b)

Figure 4: Patterns of the XRD for (a) PSi substrate, (b) GaN thin film

Table 2: The XRD patterns of porous PSi and gallium nitride/Psi

Material	2θ (Degree)	hkl	d (nm)	FWHM (Degree)	θ (Rad)	FWHM (Rad)	D (nm)	Average D (nm)	Matched by
Psi	69.82	(400)	0.13	0.7	0.609	0.012	13.8	13.8	27-1402
GaN thin Film	33.45 33.54 62.13	(002) (002) (103)	0.26 0.26 0.14	0.4 0.4 0.4	0.29 0.292 0.542	0.006 0.006 0.006	20.76 20.77 23.2	21.57	01-074-0243

4.2 Morphological results

4.2.1 Atomic force microscopy properties

Figure 5a shows images captured by atomic force microscopy (AFM) of the Psi substrate . Table 3 shows that the average diameter, roughness, and root mean square values can differ. The average diameter is 19.2 nm, the roughness of porous silicon is 5.73 nm, and the root mean square value is 7.51 nm. Figure 5b depicts GaN nanoparticles operating at a wavelength of 532 nm, exhibiting an average diameter of 29.36 nm, a roughness of 20.63 nm, and a root mean square of 27 nm. The data indicate a rise in both the roughness and root mean square. The results show that an increase in surface roughness leads to a corresponding increase in the chemical reaction, consequently enhancing the sensitivity of the gas sensor application. When we examined AFM pictures of GaN nanoparticles, we noticed that the grains were evenly spread out over the scanning area, and each grain column was facing upwards. Gallium nitride granules were dispersed over the porous silicon surface to fill the surface of the PSi. This is consistent with the results presented in two previous studies [33,34].

Table 3: The AFM measurements of the GaN/PSi and porous silicon nanostructures at a wavelength of 532 nm

Group no	Root-mean -square (nm) (RMS)	Average surface roughness (nm)	Average diameter (nm)
Psi substrate	7.51	5.73	19.2
GaN/Psi thin film	27	20.63	29.36

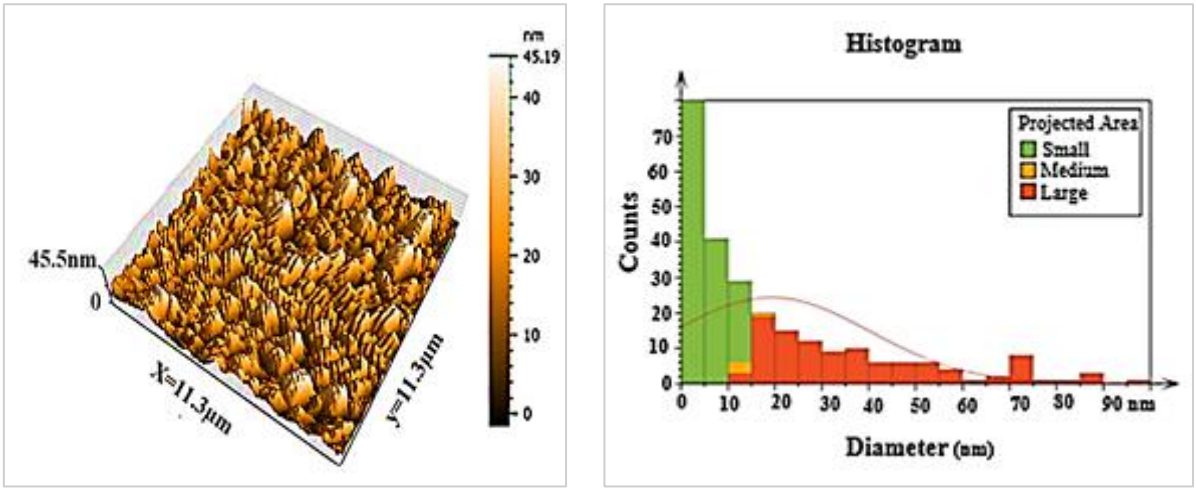

(a)

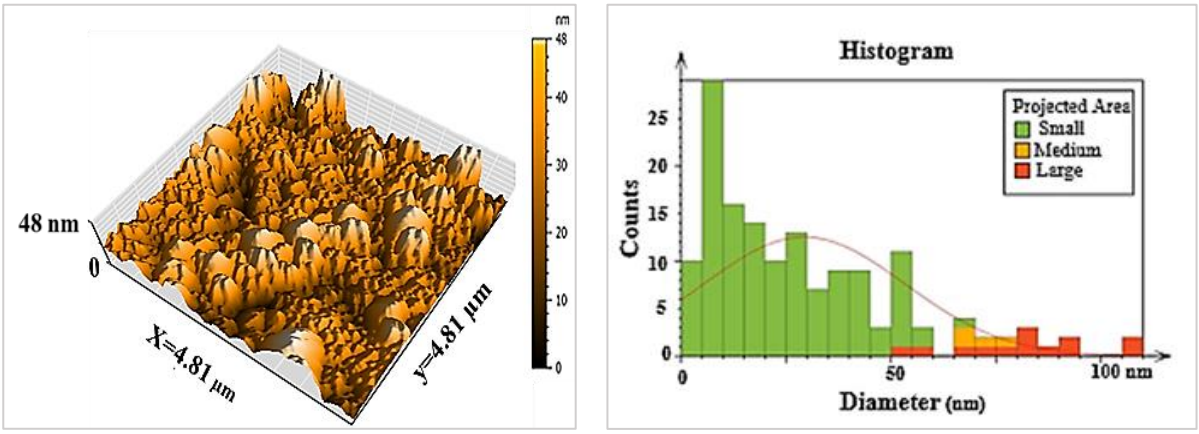

(b)

Figure 5: At 532 nm, images of AFM for (a) PSi and (b) gallium nitride/porous Si nanostructures

4.2.2 Field emission scanning electron microscopy properties

Figure 6a displays Field Emission Scanning Electron Microscopy (FE-SEM) images of porous silicon, formed via photoelectrochemical etching at a current density of 20 mA/cm², revealing elongated, uniformly shaped pores resembling stars. These pores uniformly cover the entire surface, as observed in Omar et al.'s study [35], facilitated by n-type silicon (100) with low resistivity [27]. Additionally, Figure 6b shows a cross-sectional FE-SEM image of the 100 nm thick porous silicon layer. The FESEM pictures in Figure 7a,b reveal that the GaN film, deposited at a wavelength of 532 nm, completely covers the PSi surface at different magnification (60000x and 120000x). The film exhibits a uniform and even distribution of spherical particles, which display a cauliflower morphology. The measured cross-sectional thickness of the GaN film developed at a wavelength of 532 nm was 2.92 µm, as depicted in Figure 7c.

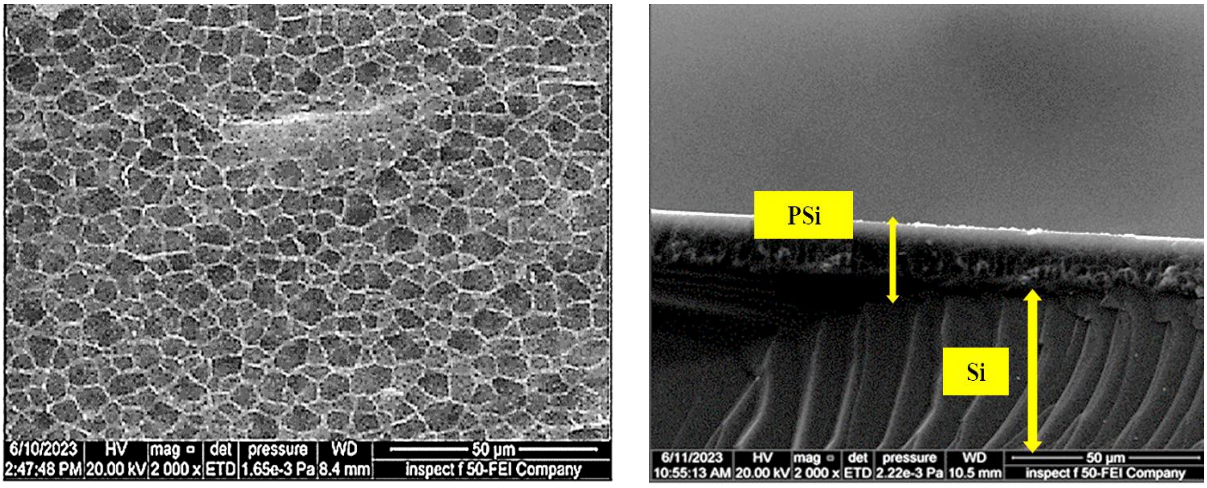

(a) **(b)**

Figure 6: The field emission scanning electron microscope (FESEM) of (a) the PSi and (b) the cross-section of the psi layer

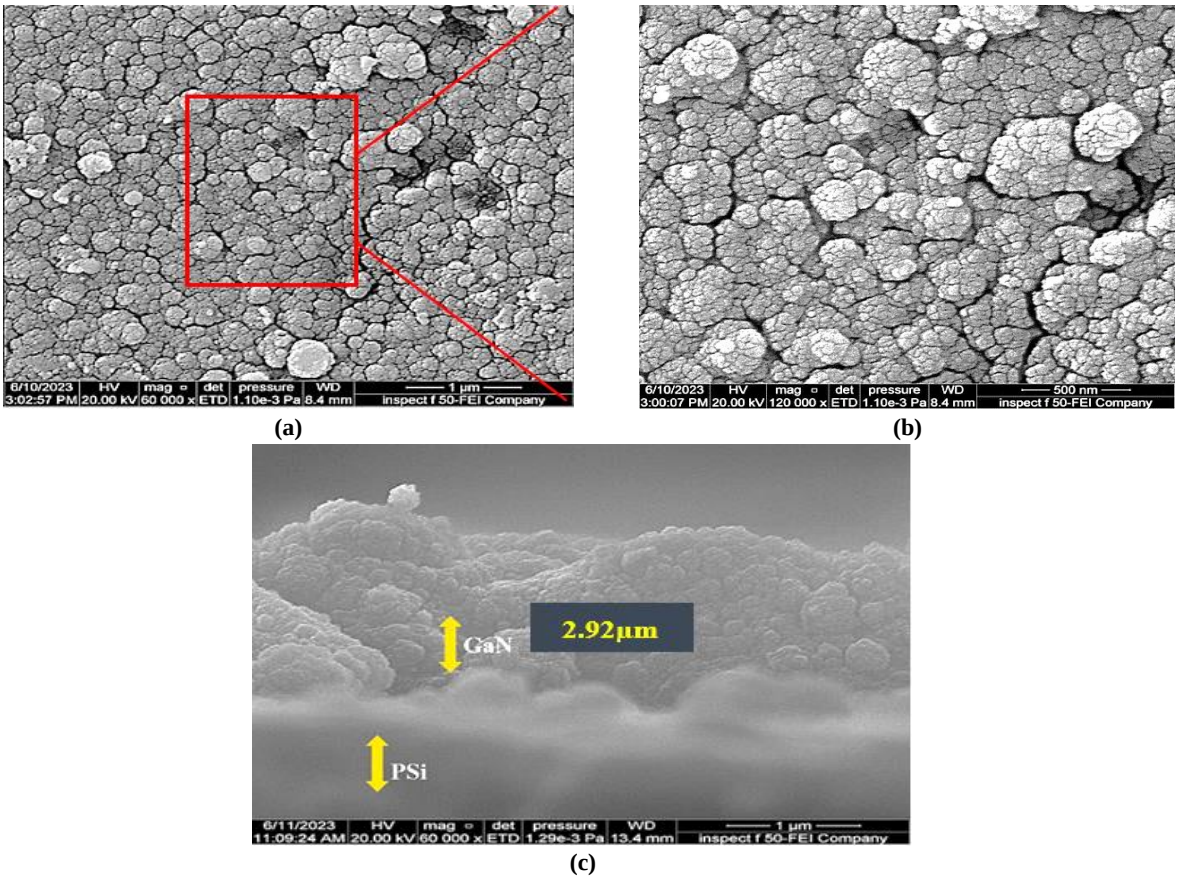

(a) **(b)**

(c)

Figure 7: FESEM images of grown GaN film at a wavelength of 532 nm, (a) magnified 60,000X, (b) magnified 120,000X, (c) FESEM cross-section image

Figure 8a shows the EDX analysis of porous silicon substrates produced at a current density of 20 mA/cm^2. The created Psi substrates were manufactured utilizing the photoelectrochemical etching process with the assistance of a diode laser. The

EDX analysis verifies the presence of O and Si as two conspicuous peaks to corroborate the composition of the substrates. Figure 8b presents spectra showing the presence of Ga and N elements, with a stoichiometric ratio of [Ga]/[N] measured at 44%, alongside a prominent Si peak from the substrate. The grid used for measurements enables the detection of background noise signals.

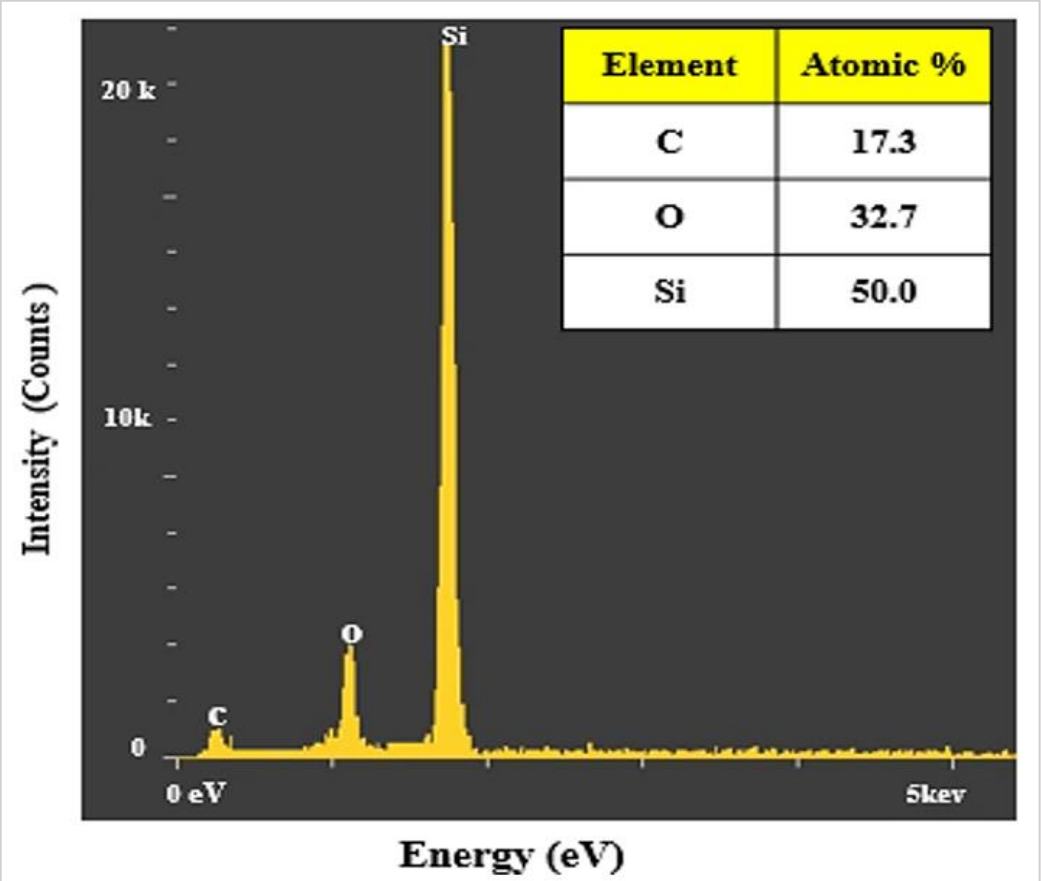

(a)

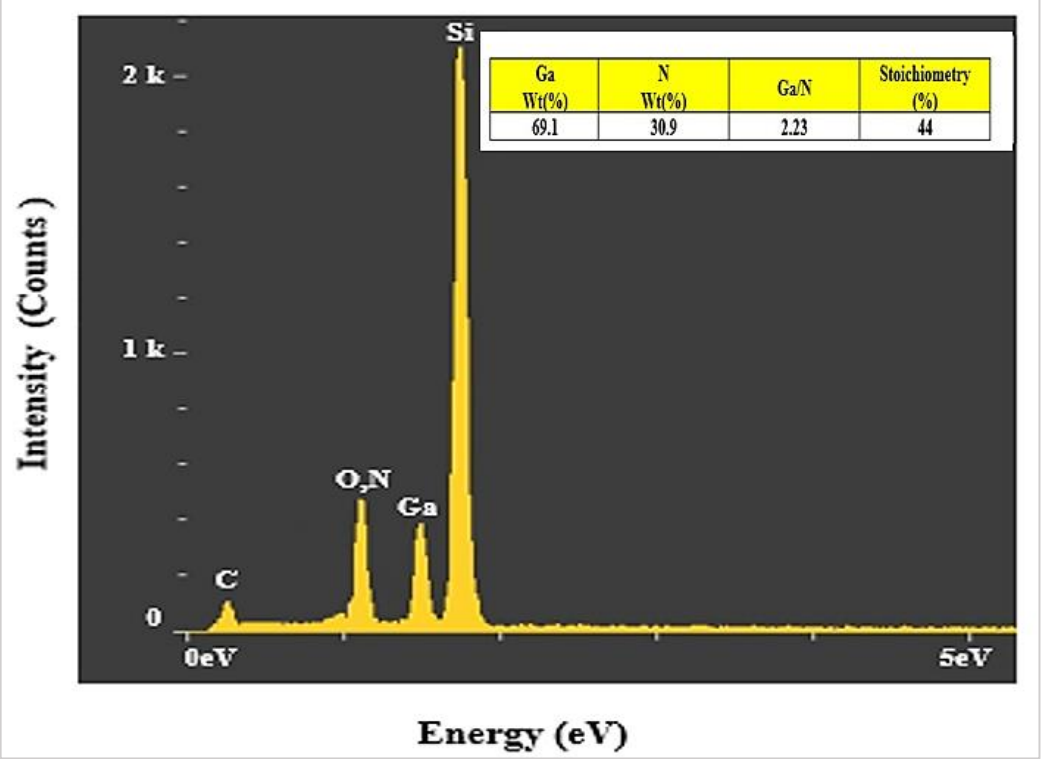

(b)

Figure 8: (a) EDX images of prepared PSi substrates by PECE method assisted by a diode laser,(b) EDX images of fabricated GaN/Psi at 532 nm

4.3 Spectroscopic properties analysis

For 9 minutes, a current density of 20 mA/cm^2 was used to etch the n-type P-Si samples and to get their photoluminescence (P.L.) spectra. The spectra obtained are shown in Figure 9a. According to Wang [34], the artificially created PSi substrate emits visible photoluminescence (P.L.) with a peak wavelength of 585 nm in the yellow spectrum. In [35], it was said that the emission came from surface states and quantum confinement that formed on the P-Si during the photoelectrochemical etching process. Additionally, we examined the GaN film's photoluminescence spectrum after it was deposited on a P-Si substrate. These can be seen in Figure 9b. The GaN layer that was detected exhibited UV photoluminescence (P.L.) with a wavelength of 363.7 nm, which signifies the existence of GaN material. Furthermore, Wang et al. [34] documented the identification of red photoluminescence (P.L.) with a wavelength peak of 723 nm, which corresponds to Psi. Li et al. [36] found changes in the photoluminescence spectrum and the energy gap after adding GaN material to the porous silicon substrate. The alteration was attributed to adjustments in the surface chemistry that occurred during the deposition procedure. The optical band gap was later analyzed using Equation 3 [37].

$$Eg(eV) = h\upsilon/\lambda = 1240/\lambda\ (nm) \quad (3)$$

where h is Planck's constant (6.62×10^{-34} J. Sec), υ is the frequency of the photons, and λ is its source wavelength, E.g. represents the energy gap.

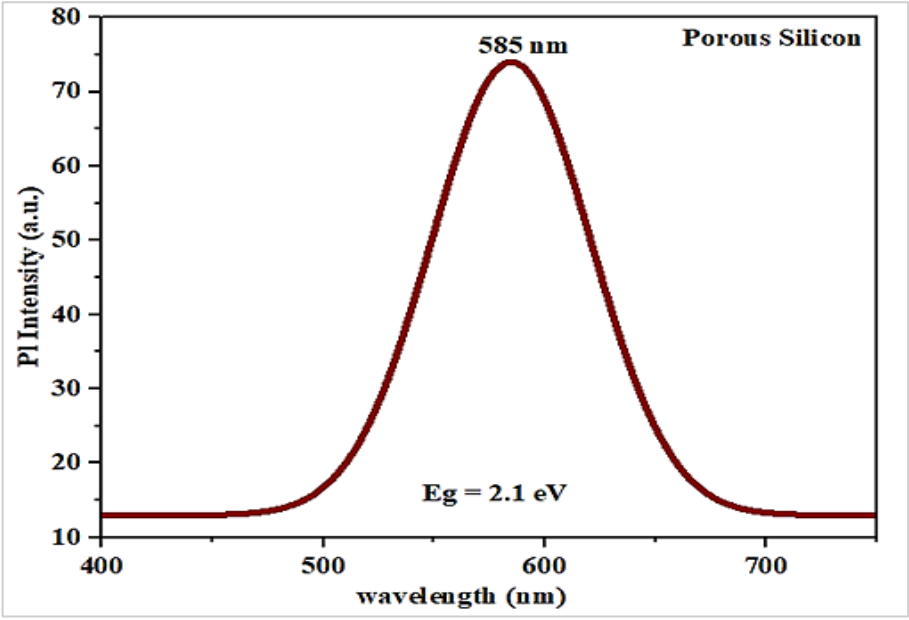

(a)

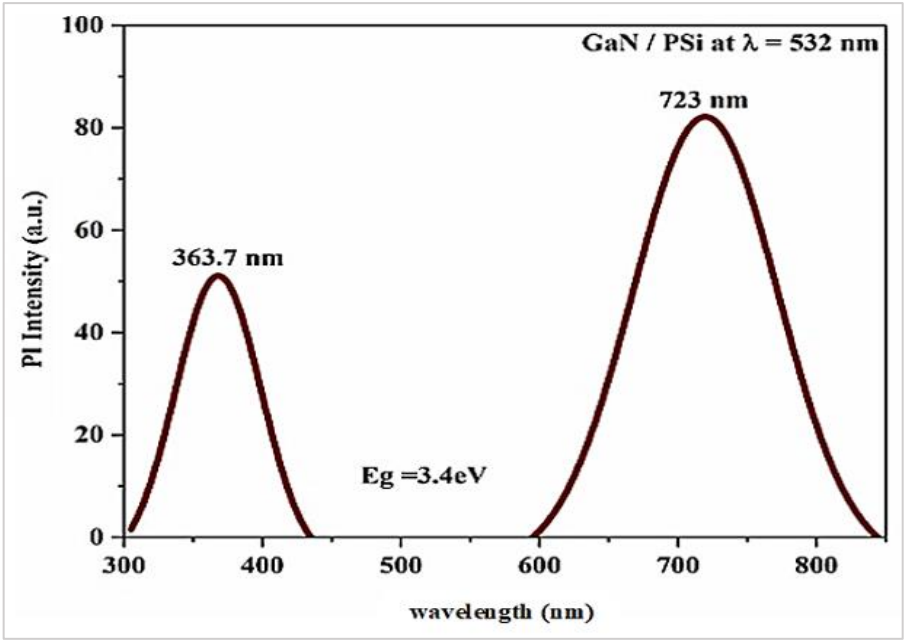

(b)

Figure 9: Photoluminescence (PL) spectra of (a) porous silicon and (b) gallium nitride were deposited on a PSi substrate

4.4 Optical results

The double-beam UV-VIS spectrophotometer was utilized to measure and quantify the optical properties, namely absorptions and absorption coefficients. The measurements were conducted throughout the wavelength range, from 200 to 1000 nm. Furthermore, the energy bandgap was calculated based on the optical energy. Utilizing Equation 4, it was possible to determine the incident photon energy. A graph illustrating the correlation between wavelengths and the absorption coefficient was generated. The formula employed to approximate the value between 32 and 33 using a factor of 4 is as follows:

$$(\alpha h\nu) = B\,(h\nu - Eg)^{r} \quad (4)$$

The absorption coefficient value (α) is computed based on the energy of the photon (hν), a constant (B), and another constant (r), whose values vary depending on the type of material. The optical band gap was determined by extrapolating a straight line from the curve relating (α hν)1/r and (hν). Equation 5 [38-41] estimated the absorption coefficient at a specific wavelength.

$$\alpha = 2.303\,(A / t) \quad (5)$$

A distinct boundary in the ultraviolet (U.V.) region guarantees the creation of direct gaps in the films made. The expression [42-44] was used to determine it as follows Equation 6:

$$\alpha h\nu = A(h\nu - Eg)^{1/2} \quad (6)$$

where hν represents the photon energy, α is the absorption coefficient, and A is a constant. The energy gap, Eg, was determined by extrapolating the linear relationship between $(\alpha h\nu)^2$ and hν to the energy of the incident photons.

Figure 10 shows the transmission spectrum of GaN/Psi thin film at 532 nm of laser wavelength. The absorption spectrum in Figure 11a ranges from 200 nm to 1000 nm and exhibits an absorption peak at approximately 221 nm. The experimental data on spectrum absorption show less broadening, which suggests that a higher concentration of GaN nano particles is linked to better absorption. A decrease in laser wavelength from 1064 nm to 532 nm led to a significant reduction in transmission values and increased absorption, indicating more ablation from the target at shorter wavelengths, resulting in higher deposition rates. This caused sample thickness to increase as the wavelength decreased, leading to increased laser-to-target absorption and a more intensive plasma plume.

Figure 11b illustrates the absorption coefficient of GaN at a laser wavelength of 532 nm. The peak relates to the wavelength at which the maximum number of photons is absorbed, while the lower values reflect a reduced absorption of photons at that particular wavelength. The prominent peak on the absorption coefficient curve signifies the insufficiency of energy in the material to induce the passage of an electron between energy levels.

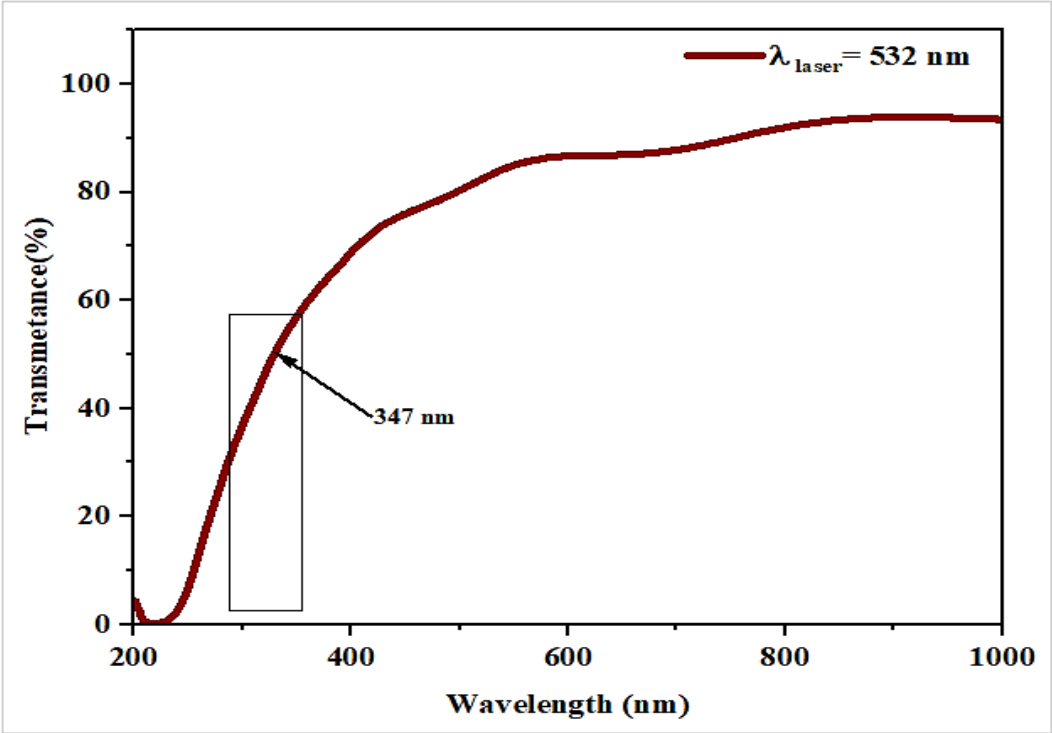

Figure 10: Transmission of GaN /psi at 532 nm of laser wavelength,900 m J, and 300 ℃

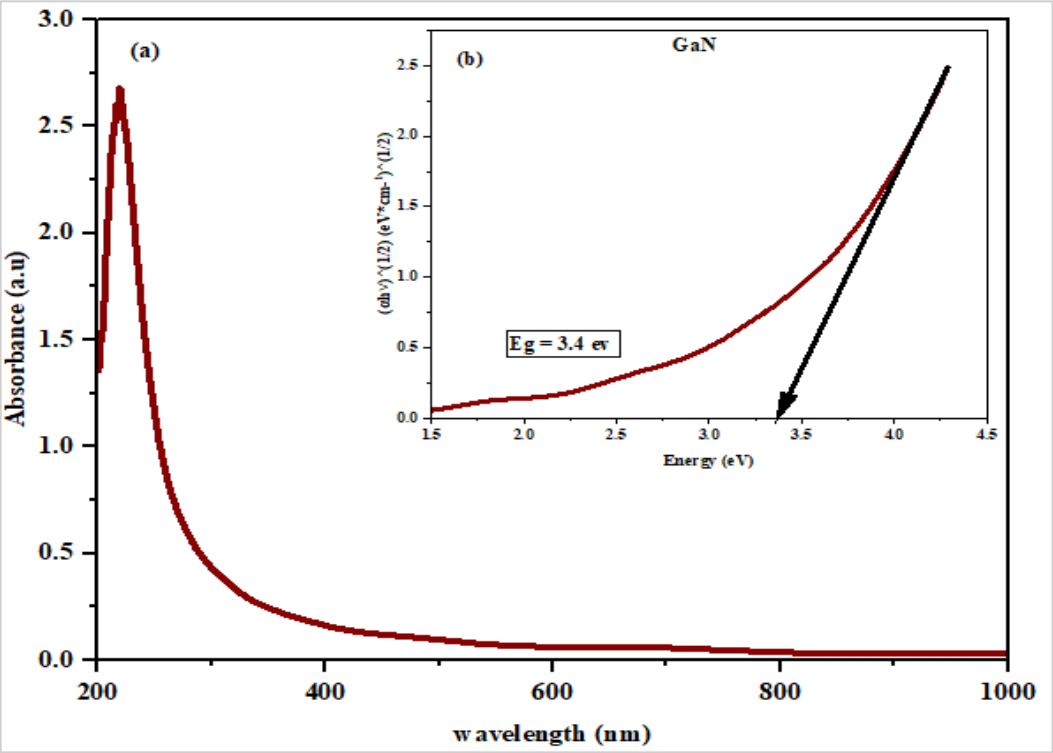

Figure 11: (a) Absorbance of GaN / Psi and (b) absorption coefficient of GaN

5. Conclusion

The GaN nanoparticles were put on the porous Si substrate using pulse laser deposition. Because of its structure, the hexagonal-GaN nanostructure can be seen and is clear at three different planes (002), (002), and (103), with a crystallite size of 21.57 nm on average. This peak aligns with the GaN crystal's hexagonal shape. The nanofilms produced exhibited a high level of uniformity in topography and surface features, with nanoparticles evenly distributed throughout. Furthermore, it was observed that crystal formation on the porous silicon substrate significantly increased the surface roughness to 20.63. The measured cross-sectional thickness of the GaN film developed at a wavelength of 532 nm was 2.92 µm. The energy band gap of the porous silicon substrate and the gallium nitride nanofilm deposited on it has been individually calculated. The direct optical energy gaps of GaN have been determined using photoluminescence (P.L.) and UV-visible spectroscopy. The PSi substrate exhibited an optical energy gap of 2.1 eV, whereas the resulting gallium nitride film displayed multiple energy band gaps of 3.4 eV and 1.7 eV. The AFM and FESEM data also provide support for this.

Author contributions

Conceptualization, A. Alwahib, and M. Fakhria; data curation, A. Abbas, and M. Fakhri; formal analysis, A. Abbas, and M. Fakhri; investigation, A. Abbas, A. Alwahib, Makram A. Fakhri, Subash C. B Gopinathb, and U. Hashim; methodology, A. Abbas, and M. Fakhria; project administration, A. Alwahib, and M. Fakhri, resources, A. Abbas, A. Alwahib, M. Fakhri, Subash C. B Gopinath, and U. Hashim; software, A. Abbas, A. Alwahib, and M. Fakhri; supervision, A. Alwahib, and M. Fakhri; validation, A. Abbas, A. Alwahib, M. Fakhri, Subash C. B Gopinath, and U. Hashim; visualization, A. Alwahib, M. Fakhri, Subash C. B Gopinath, and U. Hashim; writing—original draft preparation, A. Abbas; writing—review and editing, A. Alwahib, M. Fakhri, Subash C. B Gopinath, and U. Hashim. All authors have read and agreed to the published version of the manuscript.

Funding

This research received no specific grant from any funding agency in the public, commercial, or not-for-profit sectors.

Data availability statement

The data that support the findings of this study are available on request from the corresponding author.

Conflicts of interest

The authors declare that there is no conflict of interest.

References

[1] Gogotsi, Y. Nanomaterials handbook; CRC Press Taylor & Francis Group, 2006. https://doi.org/10.1201/9781420004014

[2] Aneesh, P. Growth and Characterization of Nanostructured Wide Band Gap Semiconductors for Optoelectronic Applications. Ph.D. Thesis, Cochin University of Science and Technology,Cochin - 682 022, Kerala, India 2010.

[3] A. Claude, G. Sankar, S. Sathya, A. Poiyamozhl, Growth of Thin Films Of Zno By Induction Heated Liquid Phase Epitaxy, Adv. Appl. Sci. Res., 4 (2013) 13–20.

[4] Buchholt, K. Nanostructured Materials for Gas Sensing Applications; Linköping University Electronic Press, Linköping, 2011.

[5] H. S. Hassan, A. B. Kashyout, I. Morsi, A. A. A. Nasser, A. Raafat, Fabrication and characterization of nano-gas sensor arrays, AIP Conf. Proc., 1653, 2015. https://doi.org/10.1063/1.4914233

[6] H. W. Kim and N. H. Kim, Preparation of Gan Films on Zno Buffer Layers By Rf Magnetron Sputtering, Appl. Surf. Sci., 236 (2004) 192–197. https://doi.org/10.1016/j.apsusc.2004.04.029

[7] T. D. Moustakas and R. Paiella, Optoelectronic Device Physics and Technology of Nitride Semiconductors From The UV To The Terahertz, Reports Prog. Phys., 80 (2017) 0–97. https://doi.org/10.1088/1361-6633/aa7bb2

[8] M. Yang, H.S. Ahn, J.H. Chang, S.N. Yi, K.H. Kim, H. Kim, S.W. Kim, Photoluminescence Investigation of Thick Gan Films Grown on Si Substrates By Hydride Vapor Phase Epitaxy, J. Korean Phys. Soc., 43 (2003) 1087–1090.

[9] W. Bdaiwi, Fabrication of Gas Sensor Device for H_2 and NO_2 from Porous Silicon, Appl. Phys. Res., 7 (2015)1-12. https://doi.org/10.5539/apr.v7n5p1

[10] R. A. Ismail, Fabrication and Characterization of Photodetector Based on Porous Silicon, e-J. Surf. Sci. Nanotech., 8 (2010) 388–391. https://doi.org/10.1380/ejssnt.2010.388

[11] S. Praveenkumar, D. Lingaraja, P. Mahiz Mathi, G. Dinesh Ram, An Experimental Study of Optoelectronic Properties of Porous Silicon for Solar Cell Application, Optik,178 (2019) 216–223. https://doi.org/10.1016/j.ijleo.2018.09.176

[12] N. A. Asli, S. F. M. Yusop, M. Rusop, S. Abdullah, Surface and Bulk Structural Properties of Nanostructured Porous Silicon Prepared By Electrochemical Etching At Different Etching Time, Ionics, 17 (2011) 653–657. https://doi.org/10.1007/s11581-011-0543-5

[13] A. Ramizy, Z. Hassan, K. Omar, Porous Silicon Nanowires Fabricated By Electrochemical and Laser-Induced Etching, J. Mater. Sci. Mater. Electron., 22 (2011) 717–723. https://doi.org/10.1007/s10854-010-0199-3

[14] S. N. Ogugua, O. M. Ntwaeaborwa, H. C. Swart, Latest Development on Pulsed Laser Deposited Thin Films for Advanced Luminescence Applications, Coatings, 10 (2020) 1–22. https://doi.org/10.3390/coatings10111078

[15] He, L. III-nitride Semiconductors Grown By Plasma Assisted Molecular Beam Epitaxy. Ph.D. Thesis, Virginia Commonwealth University Richmond, Virginia, 2004. https://doi.org/10.25772/49J8-4T47

[16] T. Zhang, T. Sugiura, W. Lu, F. Wu, J. Mao, P. Qiu, Synthesis of Gan Crystals Through The Reaction of Gallium With Lithium Amide, J. Ceram. Soc. Japan, 125 (2017) 371–374. https://doi.org/10.2109/jcersj2.16299

[17] Radzali, R. Fabrication and Characterization of Porous III-Nitrides Alloys for Application in Hydrogen Gas Sensing Devices. Ph.D. Thesis, Universiti Sains Malaysia, 2017.

[18] G. N. Chaudhari, V. R. Chinchamalatpure, S. A. Ghosh, Structural and Electrical Characterization of Gan Thin Films on Si(100), Am. J. Anal. Chem., 2 (2011) 984–988. https://doi.org/10.4236/ajac.2011.28115

[19] Woei, C. C. Rf-Mbe Grown III-Nitrides Heterostructures for Hydrogen Gas Sensing Applications. Ph.D. Thesis, Universiti Sains Malaysia, 2017.

[20] A.R. Isroi, Characteristics and Fabrication of Gallium Nitride, Conference Paper, 2015. https://doi.org/10.13140/RG.2.1.2837.9602

[21] Monteparo,C.N. Gallium Nitride Sensors for Hydrogen/Nitrogen and Hydrogen/Carbon Monoxide Gas Mixtures. M.Sc. Thesis, University of South Florida, 2009.

[22] Rajendiran, S. Plasma Enhanced Pulsed Laser Deposition. Ph.D. Thesis, University of York, 2017.

[23] Al-Rabii, I. M. A. Structural, Optical and Dielectric Properties of ($SrTiO_3$) Thin Film Prepared by PLD Technique. M.Sc. Thesis, University of Baghdad, Iraq, 2013.

[24] Mohammed, A. S. Synthesis and Characterization of Rare Earth Doped Nio Nanostructure on Si and Psi H_2S Sensor and Photodetector. Ph.D. Thesis, University of Anbar, Iraq, 2018.

[25] Heimdal, C. P. J. Pulsed Laser Deposition of Zinc Sulfide Thin Films on Silicon. M.Sc. Thesis, Norwegian University of Science and Technology, 2014.

[26] F. I. Sultan, A. A. Slman, and U. M. Nayef, IV and CV Characteristics of Porous Silicon Nanostructures By Electrochemical Etching, Eng. Technol. J., 31 (2013) 332-338. https://doi.org/10.30684/etj.31.3B.6

[27] T. Wang, X. Li, W. Feng, W. Li, C. Tao, J. Wen, Structure and Photoluminescence Properties of The Quasi-Regular Arrangements of Porous Silicon, Optoelectron. Adv. Mater. Rapid Commun., 5 (2011) 495–498.

[28] H.A.A. Abdul Amir, M.A. Fakhri, A. Alwahib, Synthesized of GaN Nanostructure Using 1064 nm Laser Wavelength by Pulsed Laser Ablation in Liquid, Eng. Technol. J., 40 (2022) 404-411 https://doi.org/10.30684/etj.v40i2.2271

[29] B. K. Kang, Y. H. Song, S. M. Kang, Y. C. Choi, D. K. Lee, Sang-Woo Kim , D. H. Yoon, Formation of Highly Efficient Dye-Sensitized Solar Cells by Effective Electron Injection with GaN Nanoparticles, J. Electrochem. Soc., 158 (2011) H693. https://doi.org/10.1149/1.3583505

[30] M. A. Qaeed, K. Ibrahim, K. M. A. Saron, A. Salhin, Cubic and Hexagonal Gan Nanoparticles Synthesized at Low Temperature, Superlattices Microstruct., 64 (2013) 70–77. https://doi.org/10.1016/j.spmi.2013.08.015

[31] F.T.L Muniz, M.R. Miranda, C. Morilla dos Santos, J.M. Sasaki, The Scherrer Equation and The Dynamical Theory of X-Ray Diffraction, Acta Crystallogr. A. Found. Adv.,72 (2016) 385-390. https://doi.org/10.1107/s205327331600365x

[32] M. A. Fakhery, Study The Properties of Silicon Nanocrystallites Prepared By Wet Etching, Eng. Technol. J., 28 (2010) 301- 306. https://doi.org/10.30684/etj.28.2.8

[33] E. T. Al Waisy, M. S. Al Wazny, Responsively, Rise Time for Bi_2O_3 /Si Photo Detector, Eng. Technol. J., 32 (2014) 33-38. https://doi.org/10.30684/etj.32.1B.5

[34] T. Wang, X. Lia, W. Feng, W. Lid, C. Taod, J. Wena, Structure and Photoluminescence Properties of The Quasi-Regular Arrangements of Porous Silicon, Optoelectron. Adv. Mater. Rapid Commun., 5 (2011) 495-498.

[35] K. Omar, K. A. Salman, Effects Of Electrochemical Etching Time on The Performance of Porous Silicon Solar Cells on Crystalline N-Type (100) and (111), J. Nano Res., 46 (2017) 45-56. http://dx.doi.org/10.4028/www.scientific.net/JNanoR.46.45

[36] K.H. Li, C. Tsai, J. Sarathy, J.C. Campbell, Chemically Induced Shifts in The Photoluminescence Spectra of Porous Silicon, Appl. Phys. Lett., 62 (1993) 3192-3194. https://doi.org/10.1063/1.109126

[37] T. Tieu, M. Alba, R. Elnathan, A. Rius, N. Voelcker, Advances in Porous Silicon–Based Nanomaterials for Diagnostic and Therapeutic Applications, Adv Ther., 2 (2019) 1800095. https://doi.org/10.1002/adtp.201800095

[38] A.S. Hassanien, A.A. Akl, Effect of Se Addition on Optical and Electrical Properties of Chalcogenide Cdsse Thin Films, Superlattices Microstruct., 89 (2016) 153-169. https://doi.org/10.1016/j.spmi.2015.10.044

[39] E. T. Salim, M. A. Fakhri, Z. Tareq, U. Hashim, Electrical and Electronic Properties of Lithium Based Thin Film for Photonic Application, AIP Conf. Proc., 2213 (2020) 20230. https://doi.org/10.1063/5.0000191

[40] M. A. Fakhri, E. T. Salim, M. H. A. Wahid, Z. T. Salim, U. Hashim, A Novel Parameter Effects on Optical Properties of The $Linbo_3$ Films Using Sol-Gel Method, AIP Conf. Proc., 2213 (2020) 20242. https://doi.org/10.1063/5.0000206

[41] R. O. Mahdi, M. A. Fakhri, E. T. Salim, Physical Investigations of Niobium Oxide Nanorod Imploring Laser Radiation, Mater. Sci. Forum, 1002 (2020) 211–220. https://doi.org/10.4028/www.scientific.net/MSF.1002.211

[42] A. A. Alwahib, S. F. Alhasan, M. H. Yaacob, H. N. Lim, M. A. Mahdi, Surface Plasmon Resonance Sensor Based on D-Shaped Optical Fiber Using Fiberbench Rotating Wave Plate for Sensing Pb Ions, Optik, 202 (2020) 163724. https://doi.org/10.1016/j.ijleo.2019.163724

[43] A. A. Alwahib, W. H. Muttlak, A. H. Abdulhadi, Multi-Response Nanowire Grating-Coupled Surface Plasmon Resonance by Finite Element Method, Int. J. Nanoelectron. Mater., 12 (2019)145–156.

[44] M. A. Fakhri, M. J. AbdulRazzaq, A. A. Alwahib, W. H. Muttlak, Theoretical Study of A Pure $Linbo_3$/Quartz Waveguide Coated Gold Nanorods Using Supercontinuum Laser Source, Opt. Mater., 109 (2020) 110363. https://doi.org/10.1016/j.optmat.2020.110363